Ten-year field evaluation of corrosion-inhibiting systems in concrete bridges barrier walls

Cusson, D.; Qian, S. Y.

Publisher's version / Version de l'éditeur:

ACI Materials Journal, 106, 3, pp. 291-300, 2009-05-01

Ten-year field evaluation of corrosion-inhibiting systems in concrete bridges barrier walls

NRCC-50550

Cusson, D.; Qian, S.Y.

May 2009

A version of this document is published in / Une version de ce document se trouve dans:
ACI Materials Journal, 106, (3), pp. 291-300

TEN-YEAR FIELD EVALUATION OF CORROSION-INHIBITING SYSTEMS IN CONCRETE BRIDGE BARRIER WALLS

Daniel Cusson and Shiyuan Qian

Biography: ACI member Daniel Cusson is a Senior Research Officer at the National Research Council of Canada, Ottawa, Ontario, Canada, K1A 0R6. He is a member of ACI Committees 363 (High-Strength Concrete) and 231 (Properties of Concrete at Early Ages), and RILEM TC 196 (Internal Curing of Concrete); and Adjunct Professor with Université de Sherbrooke, Quebec, Canada. His expertise lies in experimental testing and numerical modeling of the mechanical behavior and durability of high-performance concrete structures.

ACI member Shiyuan Qian is a Senior Research Officer at the National Research Council of Canada. He is a member of ACI Committee 222 (Corrosion of Metals in Concrete). He is also member of The Electrochemical Society and NACE International. His research interests include corrosion assessment/protection of reinforced concrete structures, corrosion inhibition, metal dissolution/passivation and hydrogen permeation/embrittlement.

ABSTRACT

The performance of eight commercial corrosion-inhibiting systems was assessed in the field over ten years on reinforced concrete barrier walls of a highway bridge that was subjected to severe environmental conditions. These systems were composed of one or more of the following components: anticorrosion concrete admixtures, reinforcement coatings, and concrete surface coatings/sealers. The field evaluation consisted of annual surveys of corrosion potential and corrosion rate, as well as visual inspections and testing of concrete cores. After ten years, the

main reinforcement of the barrier walls, at a depth of 75 mm [3 in.], was found in relatively good condition due to an initially good quality concrete. Special bars embedded at a depth of 13 mm [1/2 in.] in the barrier walls showed signs of advanced corrosion for all systems, however, no visible signs of corrosion were found on 25 mm [1 in.] deep bars. Non-destructive corrosion evaluation over the 25 mm [1 in.] deep ladder rebars indicated that the system containing the inorganic anticorrosion admixture provided consistently lower risks of corrosion, followed by systems containing organic anticorrosion admixtures, in comparison to the control system and other systems. The low concrete permeability and different stability of the protective layer forming on the bars may explain the observed differences in the effectiveness of these systems.

Keywords: bridge barrier walls; chloride ingress; corrosion-inhibiting systems; cracking; durability; high-performance concrete; steel corrosion.

INTRODUCTION

Keeping highway bridges in good condition is crucial to traffic flow and public safety. This can be a challenging task in cold climate regions where de-icing salts are used, causing reinforcement corrosion and further deterioration to concrete structures (Smith and Virmani 2000). Billions of dollars are spent every year in North America to repair concrete bridge decks (Weyers 1998; Lachemi *et al*. 2007). In order to reduce the impact of corrosion on the safety and serviceability of steel-reinforced concrete structures, measures may involve specifying the appropriate concrete mixture design, coating of the reinforcement, and/or sealing of the hardened concrete to slow down chloride penetration and reduce the rate of rebar corrosion in concrete structures. Amongst different protection techniques, corrosion-inhibiting systems are considered as one of the most promising solutions. The mechanisms by which they protect the reinforcing steel from corrosion

are often complex, as some systems delay corrosion by reducing the rate of cathodic and/or anodic reactions, while others reduce concrete permeability to chloride ions. Yet very limited data exist on the long-term performance of concrete structures built with corrosion-inhibiting systems (Elsener 2001, Chambers *et al.* 2003).

In 1996, the National Research Council of Canada (NRC) jointly with the Ministry of Transportation of Quebec (Ministère des Transports du Québec, MTQ) formed a consortium of interested partners and initiated a research project under which it was proposed to evaluate the field performance of eight proprietary corrosion-inhibiting systems applied in different sections of a barrier wall of a major highway bridge for 5 years (1996-2001). Upon completion of this initial 5-year study (Cusson *et al.* 2008), it was found that the anticorrosion admixture-based systems seemed to perform better in reducing the risk of corrosion than the systems relying on cement-based rebar coatings. However, the measured corrosion rates were found to be rather small in all test spans after the five-year period. A longer evaluation period was deemed necessary to detect significant corrosion activity and to better evaluate the long-term effectiveness of the corrosion-inhibiting systems applied on the bridge barrier wall. The corrosion assessment period was therefore extended to 2006 for a total period of ten years.

This paper presents a ten-year evaluation of the performance of corrosion-inhibiting systems under severe conditions using: (i) field corrosion testing on special rebar ladders embedded in concrete bridge barrier walls (with thin concrete covers of 13 mm [1/2 in.], 25 mm [1 in.], 38 mm [1.5 in.] and 50 mm [2 in.]) and on the main reinforcement of the bridge barrier wall (with a concrete cover of 75 mm [3 in.]); and (ii) laboratory testing of anticorrosion admixtures and rebar coatings in simulated concrete pore solutions. These combined corrosion evaluation methods

provided useful information about the effectiveness of corrosion-inhibiting systems (and some of their components) for the prevention of steel corrosion in concrete structures.

The main objectives of the present investigation were: (i) to evaluate the durability of rehabilitated concrete structures subject to the simultaneous effects of de-icing salt contamination, freeze-thaw cycles and wet/dry cycles; (ii) to better understand the factors governing the field performance of corrosion-inhibiting systems; and (iii) to identify the most effective corrosion-inhibiting systems for concrete bridge decks. A more general and long-term objective is to improve the current concrete rehabilitation technology in order to extend the service life of reinforced concrete structures in severe environments.

RESEARCH SIGNIFICANCE

Corrosion-inhibiting systems have been used over the last 20 years on concrete bridge decks to extend their service lives; however, limited test data exist on the long-term performance of concrete structures built with such systems. The selection of appropriate corrosion-inhibiting systems for specific applications remains a difficult task, since these systems may have different corrosion-inhibiting mechanisms, which effectiveness can vary depending on the test conditions. Contradictory performance results have sometimes been obtained between laboratory studies and field observations (Gulis *et al.* 1998; Qian *et al.* 2003). Documented test results from field investigations are then necessary to assess the performance of different corrosion-inhibiting systems for concrete structures, and to help bridge owners in the selection of appropriate systems depending on the given field conditions.

EXPERIMENTAL INVESTIGATION

In this section, the test structure on which the field study was conducted is described, along with a brief description of the field test program and instruments used. Additional details can be found in Cusson *et al.* (2008).

Test structure

In October 1996, the bridge owner (MTQ) undertook a major rehabilitation of Vachon Bridge in Laval (Quebec, Canada). Part of the rehabilitation work consisted of rebuilding the concrete barrier walls onto the existing concrete deck. This 6-lane wide, 714 m [2340 ft] long bridge has twenty-one 34 m [112 ft] long simple spans consisting of prestressed concrete girders supporting a reinforced concrete slab. Ten spans of the East-side concrete barrier wall were selected as the test site for the application of the commercial corrosion-inhibiting systems. As a test site, the rebuilt concrete barrier wall presented many advantages over the concrete slab (covered with membrane and asphalt), including: (a) similar initial conditions, (b) direct exposure to chlorides, and (c) easy access for instrumentation and corrosion surveys.

For this field study, ten spans of a barrier wall were built using low-permeability concrete reinforced with conventional carbon-steel reinforcement. The concrete mix had a water-cement ratio (w/c) of 0.36, and a cement content of 450 kg/m^3 [760 lb/yd^3] (CSA type 10, similar to ASTM type I). In eight of the ten test spans, corrosion-inhibiting systems with different corrosion-inhibiting mechanisms (labeled from A to H in Tables 1 and 2) were provided and installed by their respective manufacturers. The concentration of each anticorrosion admixture used in the concrete was the one recommended by its manufacturer for this type of application. Two other test spans of barrier wall were built using the same concrete (with no corrosion-

inhibiting system): one span had carbon-steel reinforcement (identified as "Control Span"), and the other span had epoxy-coated carbon-steel reinforcement (identified as "Epoxy Span"). The main reinforcement in the barrier walls consisted of eight 16 mm [5/8 in.] diameter longitudinal bars in the cross-section, and 16 mm [5/8 in.] diameter stirrups spaced at 230 mm [9 in.], as illustrated in Figure 1. The concrete typically had an air content of 6.5% and a 28-day compressive strength of 45 MPa [6530 psi]. Sensors were installed in each test section of the barrier wall to monitor temperature, relative humidity (RH) and longitudinal strain.

Field evaluation of corrosion of main reinforcement in barrier walls with normal cover

On-site non-destructive corrosion surveys of the 75 mm [3 in.] deep main reinforcement in the bridge barrier walls were performed annually during the months of May/June from 1997 to 2006 (except in 2002), including measurements of half-cell potential and corrosion rate. The front surfaces of the barrier walls were also inspected for damage due to restrained shrinkage of concrete and corrosion of the embedded reinforcement. These annual surveys were conducted under similar environmental conditions.

The half-cell potential of the reinforcement was measured according to ASTM C876 using a copper sulfate electrode (CSE) and a multimeter. The measurements were taken over three of the longitudinal reinforcing bars located at 110 mm [4.3 in.], 345 mm [13.6 in.] and 550 mm [21.7 in.] from the top of the 900 mm [35 in.] high barrier walls, and horizontally at 300 mm [12 in.] intervals over the central 15 m [49 ft.] portion of each test span. The corrosion rate (i.e. current density) of the reinforcement was measured by a *Gecor 6* device with a guard ring (manufactured by James Instruments). This instrument uses the polarization resistance technique, which consists of applying a small confined current to the reinforcing bar and measuring the change in

polarization potential. The measurements were taken on selected vertical and horizontal bars at cracked and uncracked locations in each test span.

Field evaluation of corrosion of special rebar ladders in barrier walls with reduced covers

For early detection of corrosion in the bridge barrier walls and early performance evaluation of the corrosion-inhibiting systems, two sets of rebar ladders were embedded in each test span during construction. Each rebar ladder was made of four 470 mm [18.5 in.] long horizontal bars (11 mm [7/16 in.] diameter), which were vertically spaced at 125 mm [5 in.] center to center, as shown in Figure 1. The ladder bars had varying concrete cover thicknesses, including: 13 mm [1/2 in.] for the upper bar, and 25 mm [1 in.], 38 mm [1.5 in.] and 50 mm [2 in.] for the three other horizontal bars, respectively. Measurements of half-cell potentials and corrosion rates were taken over these ladders in each test span using the same instruments and methods used for the corrosion assessment of the main reinforcement of the barrier walls.

These rebar ladders were treated in 1996 with the same corrosion-inhibiting systems used on the main reinforcement of the corresponding span, except for the set of ladders embedded in the Epoxy Span, for which ladders were made with uncoated steel reinforcement. The reason for this exception was that the quality of the epoxy coating, had it been manually installed on the ladders, would not be representative of the typical field-quality of the epoxy coating of the main reinforcement in the Epoxy Span. In fact, the presence of defects in the epoxy coating of the main reinforcement explains why it was possible to take corrosion readings on the Epoxy Span. With a defect-free epoxy coating on such ladders, the high impedance of the epoxy coating on the steel would lead to an invalid electrochemical evaluation. Therefore, the two ladders installed in the Epoxy Span can be viewed as a second pair of controls (like those installed in the Control Span).

Accelerated corrosion testing in electrochemical cells

This investigation included the assessment of: (i) effect of anticorrosion concrete admixtures on the oxidation and reduction reactions by the cyclic voltammetry method; and (ii) the effectiveness of these admixtures and cementitious rebar coatings in delaying or reducing steel corrosion by testing for chloride thresholds and corrosion rates. Working electrodes were machined from 11 mm [7/16 in.] diameter reinforcing carbon steel bars. A first group of electrodes was used to test the different anticorrosion admixtures. For the tests on rebar coatings, a second group was prepared with a 1 mm [0.04 in.] layer of a given test coating, and control electrodes were also coated with a CSA Type 10 cement paste for comparison. A saturated $Ca(OH)_2$ solution with a pH of 12.6, and a simulated concrete pore solution with a pH of 13.5 were used in this study. The anticorrosion admixtures were added to the electrochemical cells one week after the electrode samples had been immersed in the solution. Afterwards, NaCl was added to the cells and its concentration was increased weekly by 0.2% or 0.5% increments (depending on the sample) until significant corrosion developed on the electrode in order to determine the chloride threshold in the presence of each anticorrosion admixture or rebar coating. More details on the test setup for this accelerated laboratory study can be found in Qian *et al.* (2008).

RESULTS AND ANALYSES

Prevailing test conditions at the bridge

A visual inspection of the barrier walls, carried out a few days after concrete casting in 1996, revealed closely spaced vertical cracks running through the barrier walls, raising a concern for possible premature rebar corrosion due to early penetration of chlorides. These vertical cracks had an average spacing of 800 mm [31 in.]. Most cracks had an initial opening of 0.2 mm [0.008

in.] or less, with some cracks having an initial opening of 0.3 mm [0.012 in.]. Further study (Cusson and Repette 2000) confirmed that this early-age cracking was mainly due to uncontrolled thermal effects and restrained autogenous shrinkage, typical of concrete with high cement content and low water-cement ratio. It is important to say that these cracks were measured shortly after construction before the cold season. It can be expected that many of these cracks may have had widths larger than 0.2 mm during the cold season (due to thermal contraction of concrete), and later in the study due to additional drying shrinkage. With regard to chloride ingress, it is widely accepted that crack widths over 0.2 mm could lead to corrosion of the reinforcement (Pullar-Strecker 2002). However, CEB (1992) states that in the case of very severe chloride and unfavorable structural conditions, limitation of crack widths to values lower than 0.3 mm cannot prevent corrosion damage, and therefore recommends additional protection measures like rebar coating or coating of concrete.

Warm temperatures usually accelerate degradation processes, including rate of corrosion; and the moisture level in concrete also has a strong influence on reinforcement corrosion, as it affects carbonation, chloride penetration, chloride threshold, concrete electrical resistivity, and oxygen level (Vennesland *et al.* 2007). Such environmental data are therefore useful for the adequate analysis of the parameters that govern the field performance of concrete systems in corrosive environments. Fig. 2 shows typical temperatures measured at the bridge from 1997 to 2006, which varied from –10°C [14°F] or –15°C [5°F] in January to +30°C [85°F] or +35°C [95°F] in August. It can also be observed that the core concrete temperature remained at least 5°C [9°F] warmer than the ambient air temperature at any given time of the day due to the combined effect of solar exposure and the high heat capacity of concrete. Also from these data, an average number of freeze-thaw cycles was approximated to 5 cycles per year.

Fig. 3 shows the range of relative humidity monitored in the concrete barrier walls over the years (all test spans considered). It is noted that some data are missing after 2002 due to multiple power interruptions. Nevertheless, the trends in the data can still be observed. The difference between the upper and lower bounds is most likely due to the different distances between the RH/T sensors and the nearest cracks (i.e. source of moisture) and, to a lesser extent, the slightly different permeability values of the concrete systems. The RH in the barrier walls is shown to follow a seasonal pattern with high RH measured in May-June (frequent rainy periods) and low RH in December-January (cold and dry periods). Overall, the concrete RH decreased with time as a result of continual drying towards values close to 80% ± 5% after ten years. In such partially saturated concrete, oxygen can diffuse through concrete and reach the steel reinforcement. The data in Fig. 3 imply that moisture was present in sufficient quantities to provide some of the conditions leading to steel corrosion in the presence of chlorides. The risk of corrosion is usually considered low in dry concrete when RH is lower than 50% due to an impeded electrolytic process, or in saturated concrete (near 100% RH) due to low oxygen content (Tuutti 1982; ACI Committee 222, 2001).

Measured concrete properties

Table 3 presents the compressive strengths measured on 100 mm x 200 mm [4 in. x 8 in.] cores taken from the concrete barrier walls in May 1997, June 2001 and June 2006. As cement hydration took place, the overall compressive strength increased by 38% in the first four years from 45 MPa [6530 psi] to 61 MPa [8850 psi], with no significant change thereafter. Table 3 also shows that the coefficients of water vapor permeability decreased in the first 4 years and remained constant thereafter (which is consistent with the compressive strength results). The

coefficients of permeability measured in 1997 can be considered representative of moderate permeability, and those measured in 2001 and 2006 are indicative of low permeability (Neville 1996) due to continual hydration of cement. No detrimental effects from the corrosion-inhibiting systems on the concrete properties can be observed from these results.

The test data on penetrability to chloride ions (Table 3) also indicate a trend somewhat similar to that of water permeability: the values were generally higher in May 1998, with an average of 2735 Coulombs, than the values measured in June 2001 and June 2006, with averages of 1438 and 1037 Coulombs, respectively. Based on the ASTM C1202 guidelines, the following comments can be made from the 2006 chloride penetrability data: (i) the concrete systems in Spans Control, A, B, C and E had very low chloride penetrability (with values lower than 1000 Coulombs); and (ii) the systems in Spans Epoxy, D, F, G and H had low penetrability (with values between 1000 and 2000 Coulombs). It is found that some of the measured values (those above 1000 Coulombs) were higher than those normally expected for typical 0.36 w/c concrete. Their measurements could have been influenced by the presence of voids or microcracks inside some of the test samples. Nevertheless, all test systems can be regarded as having at least a relatively low penetrability to chloride ions.

The total chloride content by weight of concrete was determined on concrete cores taken from the barrier walls from 1997 to 2006, as presented in Fig. 4. The range of suggested chloride threshold values required to initiate reinforcement corrosion is also indicated in Fig. 4. This range of values is included within the chloride threshold of 0.7 kg/m^3 [1.2 lb/yd^3] by weight of concrete suggested by ACI Committee 222 (2001) and the chloride threshold of 1.4 kg/m^3 [2.4 lb/yd^3] suggested by CEB (1992) for concrete with a cement content of 350 kg/m^3 [590 lb/yd^3] and

uncoated carbon-steel reinforcement. Considering a cement content of 450 kg/m^3 [760 lb/yd^3] and a density of 2350 kg/m^3 [3960 lb/yd^3] for the concrete used in the bridge barrier wall, these chloride threshold values correspond to 0.04% and 0.08% by weight of concrete, respectively. Note, however, that these values may be higher for concretes containing anticorrosion admixtures. In general, Fig. 4 shows that chloride contents typically increased over time and decreased with depth, as expected. By 2001, at depths up to 50 mm [2 in.], the chloride contents in all test spans exceeded the range of chloride threshold values. In 2006, at depths of 50-75 mm [2-3 in.], the chloride contents were within the range of chloride threshold values in all test spans, suggesting that depassivation of the main reinforcement probably just started in uncracked concrete. However, localized pitting corrosion was likely to have developed much earlier at the transverse cracks due to the higher chloride contents readily available at the reinforcement. The concrete in all spans (except Span G) showed quite similar chloride profiles over time. The system in Span G, however, performed very well in 1997, at which time only very low chloride concentrations were measured in the concrete due to the added hydrophobic sealer at the concrete surface. In the following years, chlorides penetrated in the concrete at a significantly lower rate than in other systems. It is worth mentioning that this migrating sealer was sprayed over a thin cement-based parging applied on the front surfaces of the concrete barrier walls, which spalled off a year after installation due to severe weathering and abrasion.

Assessment of corrosion of the main reinforcement in bridge barrier walls (normal cover)

Fig. 5 presents the half-cell potential measured over the main reinforcement where each data point is an average of over a hundred readings taken during a single annual survey. In 1997, the initial average half-cell potentials were between –300 mV and –400 mV vs. CSE (except in Epoxy Span where it was less negative). In the following years, the average potentials shifted

gradually towards more negative values in all spans regardless of the presence and type of corrosion- inhibiting system. The observed negative shifts in half-cell potential may be due to a combination of the following factors: (i) the use of low-permeability concrete resulting in oxygen depletion at the reinforcement, and (ii) the presence of early-age cracks, which possibly resulted in premature pitting corrosion of the reinforcement. Spans Epoxy, A and G had the least negative average potentials in 1997 due to the high electrical resistance of their additional coating on the reinforcement and/or concrete. The positive shifts in potential observed for Spans Epoxy and A in the later years can be explained by a possible diminution of the oxygen depletion at the steel surface and a high electrical resistance, which was initially caused by the presence of the intact rebar coating. It is therefore important in the analysis to consider first the relative changes in half-cell potential over time and then its actual numerical value at a given time (Vennesland *et al.* 2007). As it is known, very negative half-cell potential readings can arise from factors other than corrosion, such as oxygen depletion in concrete being the most significant one (Qian *et al.* 2003; Elsener *et al.* 2003; Hansson *et al.* 2004).

Fig. 6 shows the cumulative distributions of the half-cell potential measurements obtained in 1997, 2001 and 2006. With time, the potentials shifted towards more negative values, indicating an increase in the risk of corrosion. The Epoxy Span showed less negative potentials compared to the other spans. This may be due to the high electrical resistance of the epoxy coating. A similar trend is seen in 2006 on Span A, for which the bars had been covered with a cementitious coating before installation in the barrier wall in 1996 (i.e. bars were electrically isolated). Not considering Spans Epoxy and A for the above reason, it is observed that all 2006 curves are within a narrow range of ±30 mV from the Control Span, suggesting that the risk of corrosion is not high enough to differentiate one system from another as far as corrosion-inhibiting effectiveness is concerned.

This is in agreement with the low chloride contents measured at a depth of 75 mm [3 in.]. It should be noted that the Control System and all the other test systems already had some form of built-in corrosion protection consisting of low permeability concrete and a 75 mm [3 in.] thick concrete cover.

Fig. 7 shows the average corrosion rate (or current density) measured over the 75 mm [3 in.] deep reinforcement at cracked and uncracked locations. Initially, the test spans with no coatings on the reinforcement showed relatively high current densities in 1997 and 1998, which were due to the formation process of a protective oxide film on the reinforcement. Afterwards, the current densities decreased in all spans (due to passivation) towards values below 0.5 $\mu A/cm^2$ [3.2 $\mu A/in.^2$], under which the corrosion rate is usually considered as being low to moderate (Rodriguez *et al.*, 1994). In general, higher corrosion rates were found at cracked locations than at uncracked locations, as expected, with an overall increase of 35% for the nine spans with non-epoxy coated reinforcement.

Assessment of corrosion of ladder bars embedded in bridge barrier walls (reduced covers)

Fig. 8 shows the half-cell potential measured on the special rebar ladders for each span from 1996 to 2006. (Note that the Epoxy System was not applied on the special ladders as explained earlier.) In all spans, it can be seen that the initial values of half-cell potential in 1996 were close to –200 mV and became more negative with time. The potential shifted towards negative values more rapidly at Bar 1 (13 mm [1/2 in.] cover) than at Bar 2 (25 mm [1 in.] cover) due to a higher chloride content near the concrete surface, as expected. The curves for Bars 2 also show that

Spans H and F had the least negative potentials in 2006 (≥ –550 mV), indicating the lowest risks of corrosion at a depth of 25 mm [1 in.], compared to the Control Span and the other test systems.

Fig. 9 presents the corrosion rates measured on the special rebar ladders for each span between 1997 and 2006. In most spans, the corrosion rates were much higher on Bar 1 (13 mm [1/2 in.] cover) than on Bar 2 (25 mm [1 in.] cover), as expected. In 2006, all corrosion rates on Bar 1 exceeded the value of 0.5 $\mu A/cm^2$ [3.2 $\mu A/in.^2$], over which corrosion can be considered active. This is in good agreement with the damage observed over Bar 1 of the rebar ladders (Table 3). On Bar 2, the 2006 values of corrosion rate for all spans (except in Spans Control and A) were below the critical value of 0.5 $\mu A/cm^2$ [3.2 $\mu A/in.^2$], which are also consistent with the lack of damage on the concrete surface over Bar 2 in 2006. The best-fit curves of corrosion rate at Bar 2 showed that Spans H and B had the lowest corrosion rates in 2006 (≤ 0.2 $\mu A/cm^2$ [1.3 $\mu A/in.^2$]) for a depth of 25 mm [1 in.]. Spans E and F also had relatively low corrosion rates (≤ 0.25 $\mu A/cm^2$ [1.6 $\mu A/in.^2$]), compared to the Control span (average of 0.47 $\mu A/cm^2$ [3 $\mu A/in.^2$]).

Assessment of corrosion-induced damage of the bridge barrier walls

As discussed before, the front surfaces of the barrier walls were inspected in June 2006 for corrosion-induced damage over the embedded rebar ladders. These observations are summarized in Table 3. A photograph of the concrete surface condition over a rebar ladder is shown for the control span (Fig. 10). Horizontal cracking was considered to be the first step in the progression of damage due to rebar corrosion (Fig. 11a), followed by delamination (Fig. 11b) and/or concrete spalling with exposed rebars (Fig. 11c). Based on the 2006 visual observations, Spans D and H were found to have the lowest degree of damage consisting only of minor horizontal cracks (as

indicated in Table 3). Nevertheless, it can be concluded, however, that corrosion was active on the first ladder bars (with a 13 mm [1/2 in.] cover) in all test spans. It is interesting to note that horizontal cracks and rust stains over the first ladder bars in Spans E and G had already been observed in 2001; however, this damage could have been triggered by the early-age vertical shrinkage cracks. Inspection of the concrete surface over the second ladder rebars (25 mm [1 in.] cover) indicated that concrete was still in good condition in all test spans in 2006 (i.e. no apparent signs of corrosion damage).

Concrete cores were taken in June 2006 over Bar 2 of each ladder to observe the corrosion of the embedded rebar. After comparing these observations with pictures of the same ladders taken before their installation in the barrier walls in 1996, it was concluded that there was no significant accumulation of additional corrosion products at the steel surface of these bars. The fact that significant concentrations of chlorides were present at this rebar level since 2001 indicates that active corrosion may soon initiate in some of these systems. However, the chloride threshold may depend on several factors such as oxygen and moisture content in the concrete, and the amount and type of anticorrosion admixture. Very little is currently known in the literature about the precise effects of these factors on the chloride threshold.

A second set of cores was taken in June 2006 over the main reinforcement of the barrier walls where the concrete cover was typically 75 mm [3 in.]. The locations of the cores were chosen to correspond to places where measurements indicated more negative corrosion potentials and higher corrosion rates. After splitting the cores, no significant corrosion was observed on these rebars, which can be expected at this depth in low permeability concrete after only ten years of exposure. This observation shows that corrosion potentials as low as –500 mV (Fig. 5) are not

always indicative of a high risk of corrosion, since oxygen content for instance may also have an influence on these readings (Vennesland *et al.* 2007).

Assessment of accelerated corrosion in corrosion cells

The long period of time usually required for evaluating the effectiveness of corrosion-inhibiting systems in reinforced concrete structures has led to the development of accelerated corrosion evaluation techniques, mainly in electrochemical cells using simulated concrete pore solutions. Many studies, however, showed that the differences in the physical and chemical properties between the simulated concrete pore solution and the actual concrete might affect differently the chemical reactions involved in reinforcement corrosion and the corrosion-inhibiting process (Hausmann 1967; Treadaway and Russel 1968; Gouda and Halaka 1970; Andrade *et al.* 2001).

A summary of the main findings of the laboratory study of accelerated corrosion is presented in this section; however, the complete investigation results can be found in Qian *et al.* (2008). This information is provided here to give additional insights on the different corrosion-inhibiting mechanisms (Table 2) used by the active ingredients included in the investigated corrosion-inhibiting systems installed in the field.

Saturated $Ca(OH)_2$ solutions (pH of 12.6) provide a good simulation of old/carbonated concretes, or new concretes containing about 10-30% silica fume. It was found that Admixtures E, H and C obtained chloride thresholds of 8%, 6% and 4% NaCl, respectively, which were higher than the 2% value obtained for the control (no admixture in solution). Admixtures B and F obtained low chloride thresholds of 0.7% and 1.1% NaCl, respectively. Coatings A, D, and G provided good

performance in the saturated $Ca(OH)_2$ solution by increasing the chloride threshold and reducing the corrosion rate of the reinforcing bars when compared to the control cementitious coating.

Simulated concrete pore solutions (pH of 13.5) provide a close simulation of new Portland cement concrete. The effectiveness of the anticorrosion admixtures in increasing the chloride threshold could not be observed, since most thresholds were 6% NaCl including the control. This is explained by the high hydroxide concentration dominating the corrosion initiation process in high pH solutions (Hussain 1996, Kayyali 1995), thus leading to a reduced apparent effectiveness of the anticorrosion admixture.

Finally, the obtained cyclic voltammograms indicated that the anodic and cathodic currents were reduced significantly in the presence of organic Admixtures E, C, and F, which may be due to the adsorption of organic compounds on the steel electrode. With the inorganic Admixture H, these currents were increased to possibly enhance the passive film formation on the steel electrode.

From the above findings, it can be observed that some of these components showing excellent performance in the laboratory did not necessarily outperform the control system when their corresponding corrosion-inhibiting systems were evaluated in the bridge barrier wall with the 75 mm [3 in.] cover. It is thus challenging to find good correlation between corrosion test results conducted under different conditions (i.e. laboratory vs. field).

DISCUSSION ON OVERALL PERFORMANCE OF TEST SYSTEMS

Performance evaluation of corrosion-inhibiting systems is a challenging task because they involve different mechanisms with varying effectiveness depending on the test conditions. This is

why in this study several different tests were conducted under both field and laboratory conditions. It should be emphasized that the performance measured or observed in the field is of prime importance compared to that found in the laboratory under controlled conditions. The laboratory tests have been conducted in parallel to identify the corrosion-inhibiting mechanisms involved and to provide supporting information to the corresponding field evaluation.

In the field study, the performance improvements of the corrosion-inhibiting systems over the control system were not as obvious as those observed in the laboratory study conducted in the electrochemical cells with the low pH solution. The high alkalinity of the relatively new concrete used in the barrier walls, the low concrete permeability, and the concrete cover of 75 mm [3 in.] are factors explaining the delay in the initiation of corrosion in concrete. Moreover, some differences should be expected when comparing test results from single anticorrosion admixtures or rebar coatings in synthetic laboratory solutions to those obtained on multi-component corrosion-inhibiting systems in the field, since complex combinations of the following factors are usually found in the field: concrete cracking, stress in the reinforcement, freeze-thaw and wet-dry cycles, periodic application of de-icing salts, carbonation, and the presence of sealers and coatings in the system, which can hardly be reproduced simultaneously in the laboratory.

The laboratory tests performed on the concrete cores taken from the barrier walls show that the concretes used for the control and the corrosion-inhibiting systems was of very good quality with low permeability to water and chlorides and good compressive strength. With the 75 mm [3 in.] concrete cover over the main reinforcement, the barrier wall in each test span already had a good built-in protection system against corrosion. The corrosion-inhibiting systems used in this study

should therefore be regarded as a second line of defense against corrosion of the reinforcement, which is particularly useful where concrete is cracked.

The assessment of the corrosion-induced damage of the front surfaces of the concrete barrier walls over the top ladder rebars (13 mm [1/2 in.] cover) indicated that corrosion was active in all test spans, with lower degrees of damage on Span H and D (few minor horizontal cracks). Inspection of the concrete cores taken over the second ladder rebars (25 mm [1 in.] cover) and over the main reinforcement (75 mm [3 in.] cover) showed no evidence of advanced corrosion in any of the systems.

In order to find some differences in the effectiveness of these corrosion-inhibiting systems, the non-destructive evaluation results taken over Bar 2 of the special ladders (where corrosion may be already active or about to become active) can provide some additional information, from which it seems that System H (inorganic anticorrosion admixture) obtained consistently good performance results (in the lab too), followed closely by Systems B, E and F (organic anticorrosion admixtures). The observed differences in the field performance of these systems may be explained as follows:

In chloride-contaminated concrete, the iron from the reinforcement forms soluble light green complexes with the chloride ions at the steel surface. These soluble complexes are able to migrate away from the reinforcing bars, thus facilitating the dissolution of iron, which leads to the breakdown of the protective passive layer on the steel bars (Foley 1975). When an inorganic admixture, such as calcium nitrite, is used in concrete, the nitrites contained in the admixture

compete with the chloride ions for the ferrous ions at the anode to form a film of ferric oxide, as shown in the reaction equations below (Soylev and Richarson 2008):

$$2Fe^{2+} + 2OH^- + 2NO_2^- \longrightarrow 2NO + Fe_2O_3 + H_2O$$

$$Fe^{2+} + OH^- + NO_2^- \longrightarrow NO\uparrow + \gamma\text{–}FeOOH$$

These reactions are much more rapid than the transport of ferrous ions via chloride ion complex formation. As a result, nitrite ions contribute to the formation of a stable passive layer, even in the presence of chloride ions. If the nitrite ion concentration is sufficiently high, then nitrite ions react with ferrous ions to form a stable passive layer that closes off the iron surface, stopping further corrosion reaction.

In the case of organic admixtures, such as those containing amines and alkanolamines (AMA), these admixtures inhibit corrosion by forming an organic protective film on the steel surface. In concrete with high permeability, polarization resistance increases with AMA content due to the formation of the protective film, as expected. In low permeability concrete, some previous laboratory studies found that polarization resistance decreased with AMA content, which was attributed to the formation of a non-stable film on the reinforcement due to the large film thickness (Dhouibi 1998; Soylev and Richardson 2008).

SUMMARY AND CONCLUSIONS

The field performance of ten 34 m [112 ft] long spans of a reconstructed bridge barrier wall protected with nine proprietary corrosion-inhibiting systems and one control system were

evaluated over ten years. The bridge was exposed to a severe climate with temperatures varying from –15°C [5°F] to 35°C [95°F] and repeated exposures to de-icing salts and freeze/thaw cycles. The field performance of the corrosion-inhibiting systems was evaluated mainly from measurements of half-cell potential and corrosion rate and from inspections of the concrete surface and cored rebars. The long period of time, normally required to evaluate the effectiveness of corrosion-inhibiting systems in concrete structures, necessitated the use of accelerated corrosion testing in electrochemical cells using simulated concrete pore solutions and on the actual structure using special embedded rebar ladders with reduced concrete covers. The major conclusions of this field investigation are summarized as follows:

1. The concrete properties measured on cores taken from the barrier walls were representative of concrete of a potentially good quality, with a compressive strength exceeding the 35 MPa [5000 psi] design requirement, and a low concrete permeability to water and chlorides. In general, these properties showed a significant improvement until about four years of age due to continual cement hydration, and then remained fairly constant thereafter.

2. The severe early-age vertical cracking observed in the barrier walls was mainly due to uncontrolled autogenous shrinkage, and thermal expansion under restrained conditions. This cracking allowed early ingress of chlorides to the reinforcement, resulting in premature localized corrosion at the cracks.

3. Total chloride contents measured after ten years at a depth of 50-75 mm [2-3 in.] in uncracked concrete remained below or near the critical chloride threshold of 0.08% by weight

of concrete in all test spans. This suggests that the risk of corrosion of the 75 mm [3 in.] deep main reinforcement was low at uncracked locations due to the low concrete permeability.

4. The migrating sealer of System G performed very well in 1997, at which time only very low chloride concentrations were measured in the concrete. In the following years, more chlorides penetrated into the concrete but at a significantly lower rate than in other systems that did not have a sealer on the barrier wall surface.

5. Field evaluation of corrosion over the 75 mm [3 in.] deep main reinforcement showed that no substantial active corrosion occurred after ten years of service. Therefore, no major differences in effectiveness could be observed between a given corrosion-inhibiting system and the control system. It should be noted that all the test systems of this study already had some form of built-in corrosion protection, as they were made of a low permeability concrete with 75 mm [3 in.] thick concrete cover.

6. Corrosion rates on the main reinforcement measured over the early-age vertical shrinkage cracks were consistently higher than those measured over uncracked locations, regardless of the corrosion-inhibiting systems used (including the system with epoxy-coated reinforcement). This pitting corrosion, localized at the cracks, did not seem to have initiated active generalized corrosion of the main reinforcement after ten years.

7. Field evaluation of the corrosion over the 25 mm [1 in.] deep ladder rebars indicated that System H (inorganic anticorrosion concrete admixture) obtained consistently good performance results (reduced risk of corrosion), followed by Systems B, E and F (organic

anticorrosion concrete admixtures), in comparison to the control system and other test systems. The low concrete permeability and different stability of the protective layer forming on the steel bars may explain the observed differences in the effectiveness of these systems.

8. Corrosion-induced damage at the barrier wall surface over the 13 mm [1/2 in.] deep bars of the embedded ladders was found in all spans, with the least damage found on Spans H and D. (Note that the Epoxy System was not tested on the special rebar ladders.)

9. Visual inspection of concrete cores taken over the 25 mm [1 in.] deep ladder bars and the 75 mm [3 in.] deep main reinforcement showed no significant corrosion in all test spans. This is due to the low water permeability concrete used in the construction of the barrier walls. This finding shows that highly negative half-cell potentials (e.g. from –500 mV to –600 mV) can be measured in non-corroded areas, as these readings can also be influenced significantly by oxygen content, for example.

ACKNOWLEDGEMENTS

The financial and technical contributions of all our project partners are gratefully acknowledged, including: Ministère des transports du Québec (MTQ), Axim-Italcementi Group, Caruba Holdings, Cortec Corporation, Euclid Admixture Canada, Israel Richler Trading, Master Builders Technologies, Sika Canada, W.R. Grace & Co., and NRC's Industrial Research Assistance Program. The sustained assistance of Louis-Marie Bélanger and Daniel Vézina from MTQ is also gratefully acknowledged. The authors would also like to thank Noel Mailvaganam, Roger Willoughby, Nathalie Chagnon, Mark Arnott, Gordon Chan and Mark Lowery from NRC for their valuable assistance.

REFERENCES

1. ACI Committee 222, *Protection of Metals in Concrete Against Corrosion*, American Concrete Institute, Farmington Hills, 2001, 41 p.
2. Andrade, C., Keddam, M., Nóvoa, X.R., Pérez, M.C., Rangel, C.M. and Takenouti, H., "Electrochemical Behaviour of Steel Rebars in Concrete: Influence of Environmental Factors and Cement Chemistry," *Electrochimica Acta*, Vol. 46, 2001, p. 3905-3912.
3. ASTM C39, *Standard Test Method for Compressive Strength of Cylindrical Concrete Specimens*, ASTM International, West Conshohocken, PA., 5 p.
4. ASTM C114, *Standard Test Method for Chemical Analysis of Hydraulic Cement*, ASTM International, West Conshohocken, PA., 30 p.
5. ASTM C876, *Standard Test Method for Half-cell Potentials of Uncoated Reinforcing Steel in Concrete*, ASTM International, West Conshohocken, PA., 6 p.
6. ASTM C1202, *Standard Test Method for Electrical Indication of Concrete's Ability to Resist Chloride Ion Penetration*, ASTM International, West Conshohocken, PA., 6 p.
7. ASTM E96, *Standard Test Method for Water Vapor Transmission of Materials*, ASTM International, West Conshohocken, PA., 8 p.
8. CEB, *Design Guide for Durable Concrete Structures*, 2nd ed., Thomas Telford Publishers, 1992.
9. Chambers, B.D., Taylor, S.R., Lane, D.S., "An Evaluation of New Inhibitors for Rebar Corrosion in Concrete," *Report VTRC 03-R8*, Virginia Transportation Research Council, 2003, 61 p.

10. Cusson, D., Qian, S., Chagnon, N.: Corrosion Inhibiting Systems for Durable Concrete Bridges – Part 1: Field Performance Evaluation, *ASCE Journal of Materials*, Vol. 105, No. 1, January 2008.
11. Cusson, D., Repette, W., "Early-age Cracking in Reconstructed Concrete Bridge Barrier Walls," *ACI Materials Journal*, Vol. 97, No. 4, July/August 2000, p. 438-446.
12. Dhouibi, L., Triki, E., Raharinaivo, A. "Laboratory experiments for assessing the effectiveness of inhibitors against steel corrosion in concrete," *Proceeding of the 6th Intl. Symposium on Advances in Electrochemical Science and Technology*, Chennai, India, 1998.
13. Elsener, B., "Corrosion Inhibitors for Steel in Concrete: State-of-the-Art Report," *Publication Number 35 of the European Federation of Corrosion*, The Institute of Material, ed., 2001, 68 p.
14. Elsener, B., Andrade, C., Gulikers, J., Polder, R., Raupach, M., "Half-Cell Potential Measurements - Potential Mapping on Reinforced Concrete Structures," *Materials and Structures*, Vol. 36, August-Sept. 2003, p. 461-471.
15. Foley, R.T., "Complex Ions and Corrosion", *Journal of the Electrochemical Society*, Vol. 11, No. 122, 1975, p. 1493.
16. Gouda, V. K., and Halaka, W. Y., "Corrosion and Corrosion Inhibition of Reinforcing Steel. II: Embedded in Concrete". *Brit Corrosion*, Vol. 5, No. 5, 1970, p. 204-208.
17. Gulis, E.W., Lai, D., Tharambala, B, "Performance and Cost Effectiveness of Substructure Rehabilitation/Repair Strategies,"*Draft Report*, Ministry of Transportation of Ontario, Downsview, Canada, 1998.
18. Hansson, C.M., Seabrook, P.T., Marcotte, T.D., "In-Place Corrosion Monitoring," *Concrete International*, Vol. 26, No. 7, July 2004, p. 59-65.

19. Hausmann, D.A., "Steel corrosion in concrete: How does it occur?" *Materials Protection*, Vol. 6, No. 11, November 1967, p. 19-23.
20. Hussain, S. E., Al-Gahtani, A. S., Rasheeduzzafar, "Chloride Threshold for Corrosion of Reinforcement in Concrete", *ACI Materials Journal*, Nov.-Dec. 1996, p. 534-538.
21. Kayyali, O. A., Haque, M. N., "The Cl/OH Ratio in Chloride-Contaminated Concrete – A Most Important Criterion", *Magazine of Concrete Research*, 1995, Vol. 47, No. 172, p. 235-242.
22. Lachemi, M., Hossain, K.M.A., Ramcharitar, M., Shehata, M., "Bridge Deck Rehabilitation Practices in North America," *ASCE Journal of Infrastructure Systems*, Sept. 2007, p. 225-234.
23. Neville, A. M., *Properties of concrete*, 4th ed., John Wiley & Sons, Inc., ed., New-York, 1996, 844 p.
24. Pullar-Strecker, P., *Concrete reinforcement corrosion – ICE design and practice guide*, Thomas Telford Ltd., ed., London, 2002, 100 p.
25. Qian, S., Cusson, D., Chagnon, N., "Evaluation of Reinforcement Corrosion in Repaired Concrete Bridge Slabs - A Case Study," *Corrosion*, Vol. 59, No. 5, May 2003, p. 457-468.
26. Qian, S., Cusson, D., Chagnon, N., "Corrosion Inhibiting Systems for Durable Concrete Bridges – Part 2: Accelerated Laboratory Investigation, " *ASCE Journal of Materials*, Vol. 105, No. 1, January 2008.
27. Rodriguez, J., Ortega, L.M., Garcia, A.M., "Assessment of Structural Elements with Corroded Reinforcement," *International Conference on Corrosion*, Sheffield, U.K., July 1994, 16 p.

28. Smith, J.L. and Virmani, Y.P., "Materials and Methods for Corrosion Control of Reinforced and Prestressed Concrete Structures in New Construction," *Report No. FHWA-RD-00-081*, FHWA, August 2000, 82 p.

29. Soylev, T.A., and Richardson, M.G., “Corrosion Inhibitors for Steel in Concrete: State-of-the-art Report, ” *Construction and building Materials,* Vol. 22, 2008, p. 609-622.

30. Treadaway, K.W. and Russel, A.D., "Inhibition of the corrosion of steel in concrete - Part 2," *Highways and Public Works*, Vol. 36, 1968, p. 40-41.

31. Tuutti, K., “Corrosion of Steel in Concrete”, *Ph.D. Thesis*, Swedish Cement and Concrete Research Institute, Stockholm, Sweden, 1982, 469 p.

32. Vennesland, O., Raupach, M., Andrade, C., "Recommendation of Rilem TC 154-EMC: Electrochemical Techniques for Measuring Corrosion in Concrete – Measurements With Embedded Probes," *Materials and Structures*, No. 40, 2007, p. 745-758.

33. Weyers, R.E., “Service life model for concrete structure in chloride laden environments”, *ACI materials journal*, Vol. 95, No. 4, July-August 1998, p. 445-453.

List of tables:

List of Figures:

TABLES AND FIGURES

Table 1–Generic description of investigated corrosion-inhibiting systems†

Name	Type	Active chemicals
Control	- Carbon-steel reinforcement	
Epoxy	- Epoxy-coated reinforcement	
A	- Rebar coating - Concrete coating	- Water-based blend, Portland cement, silica sand - Polymer-based blend, Portland cement, aggregates
B	- Organic anticorrosion admixture - Coating on anchor bars from slab	- Alkanolamines - Water-based epoxy, Portland cement
C	- Organic/inorganic admixture	- Amine derivatives, sodium nitrite
D	- Rebar coating	- Water-based epoxy, cementitious components
E	- Organic anticorrosion admixture	- Amines and esters
F	- Organic anticorrosion admixture	- Alkanolamines and amines and their salts with organic/inorganic acids
G	- Organic anticorrosion admixture - Coating on anchor bars from slab - Concrete sealer	- Alkanolamines, ethanolamine, phosphate - Water-based epoxy, Portland cement - Water-repellent penetrating silane
H	- Inorganic anticorrosion admixture	- Calcium nitrite

† Commercial names are not identified to maintain the anonymity of the manufacturers.

Table 2. General mechanisms of the anticorrosion concrete admixtures

Name	Mechanism
B, G	Blocks both the anodic and cathodic reactions by depositing a physical barrier in the form of a protective layer on the reinforcing steel.
C	Forms a protective barrier stabilizing the passivating oxide layer on the reinforcing steel. Also lowers penetration of chloride ions by increasing the cement paste density.
E	Promotes the adsorption of a film-forming amine on the reinforcing steel and the formation of a physical barrier against chloride ions. Also reduces concrete permeability.
F	Migrates in concrete and adsorbs on steel surface to form a film blocking both the anodic and cathodic reactions.
H	Enhances passivity by oxidizing ferrous ions to ferric ions and blocking the transport of ferrous ions into the electrolyte. Reacts with anodic corrosion products competing with chloride ions.

Table 3–Measured concrete properties and observed field conditions
(1 MPa = 145 psi; 1 m/s = 3.28 ft/s)

Name	Compr. strength of cored samples, ASTM C39 (MPa)			Water permeability of cored samples, ASTM E96 (m/s x 10^{-12})			Cl^- Penetrability of cored samples, ASTM C1202 (Coulombs)			Concrete wall surface condition over the 1st ladder rebar (13 mm [1/2 in.] depth)
	May 1997	June 2001	June 2006	May 1997	June 2001	June 2006	May 1998	June 2001	June 2006	June 2006
Control	41	59	56	17.2	7.0	9.6	2543	1518	576	Cracks, delamination
Epoxy	43	n/a	62	15.4	7.1	8.0	n/a	n/a	1825	n/a
A	43	64	55	13.9	6.7	6.8	1978	1159	666	Cracks, delam., spalling
B	46	68	66	12.8	5.6	6.1	2864	1365	782	Cracks, delam.
C	38	50	54	10.7	4.6	5.5	2514	1283	767	Cracks, delam., spalling
D	39	54	59	12.3	6.7	6.4	3669	1807	1447	Cracks
E	45	69	58	11.5	4.3	4.5	1555	764	927	Cracks, delam., spalling
F	45	60	56	15.9	8.7	7.2	3259	1420	1152	Cracks, delam., spalling
G	50	68	51	14.9	6.2	9.1	3626	1304	1096	Cracks, delam.
H	55	60	69	14.1	7.3	8.8	2606	2319	1134	Cracks
Average	45	61	59	13.9	6.4	7.2	2735	1438	1037	

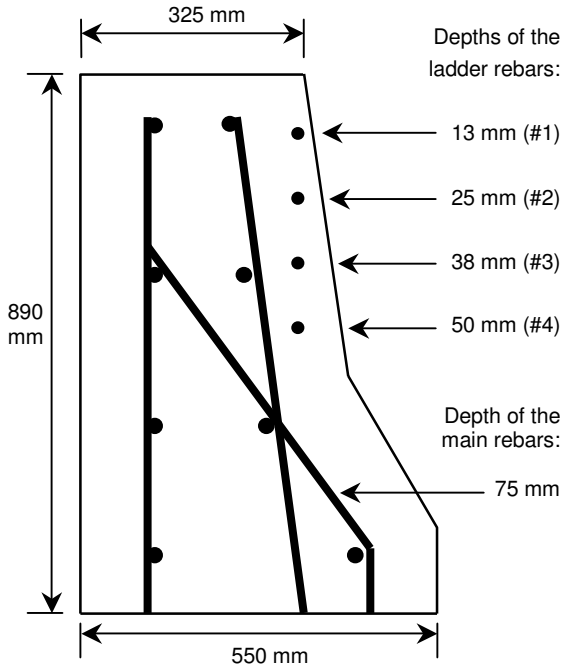

Fig. 1–Cross-section of typical test span of concrete barrier wall
(Each test span has a length of 34 m [112 ft] and includes two sets of rebar ladders)

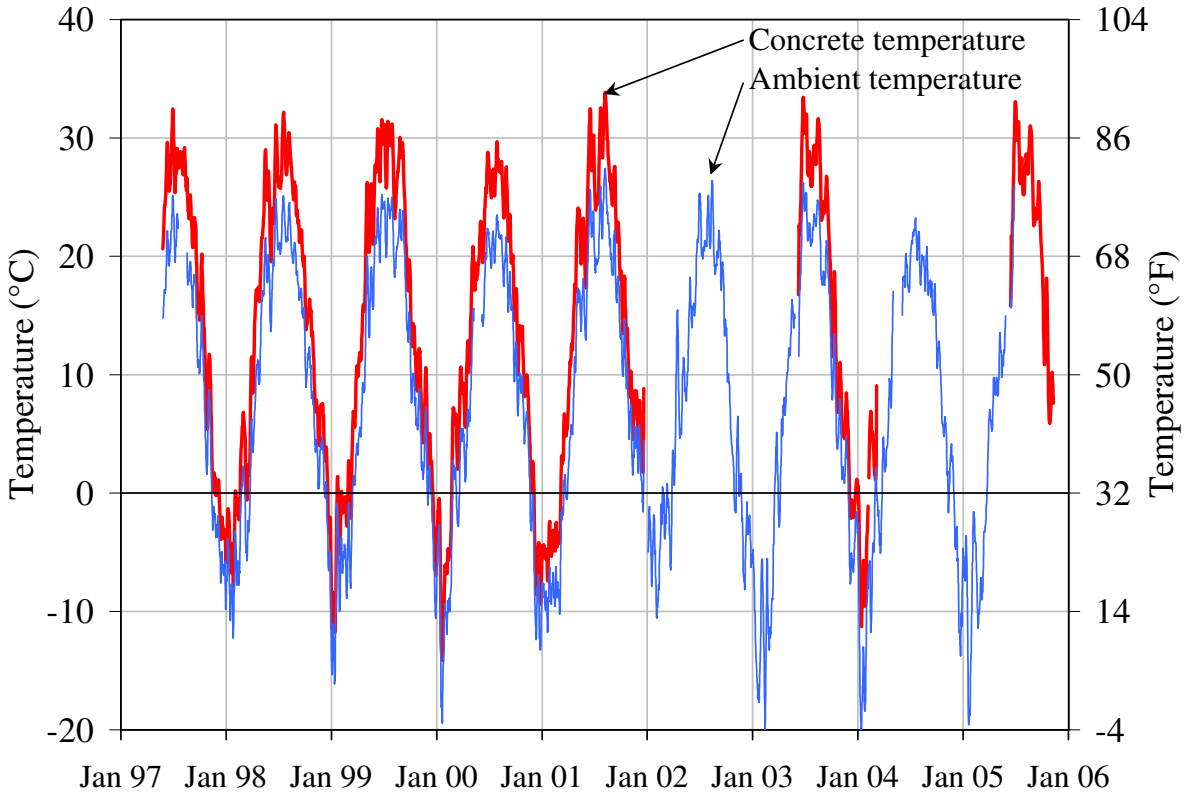

Fig. 2–Typical temperatures monitored at the bridge

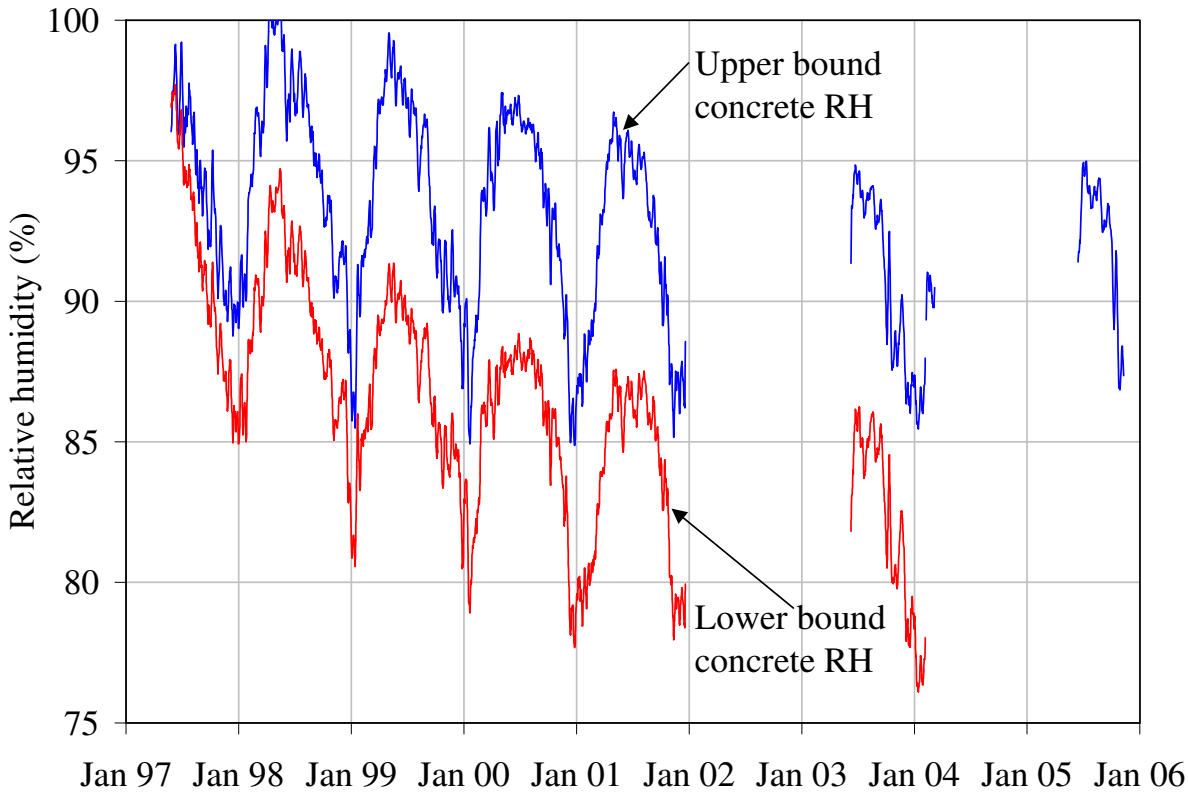

Fig. 3–Range of relative humidity monitored in concrete barrier walls

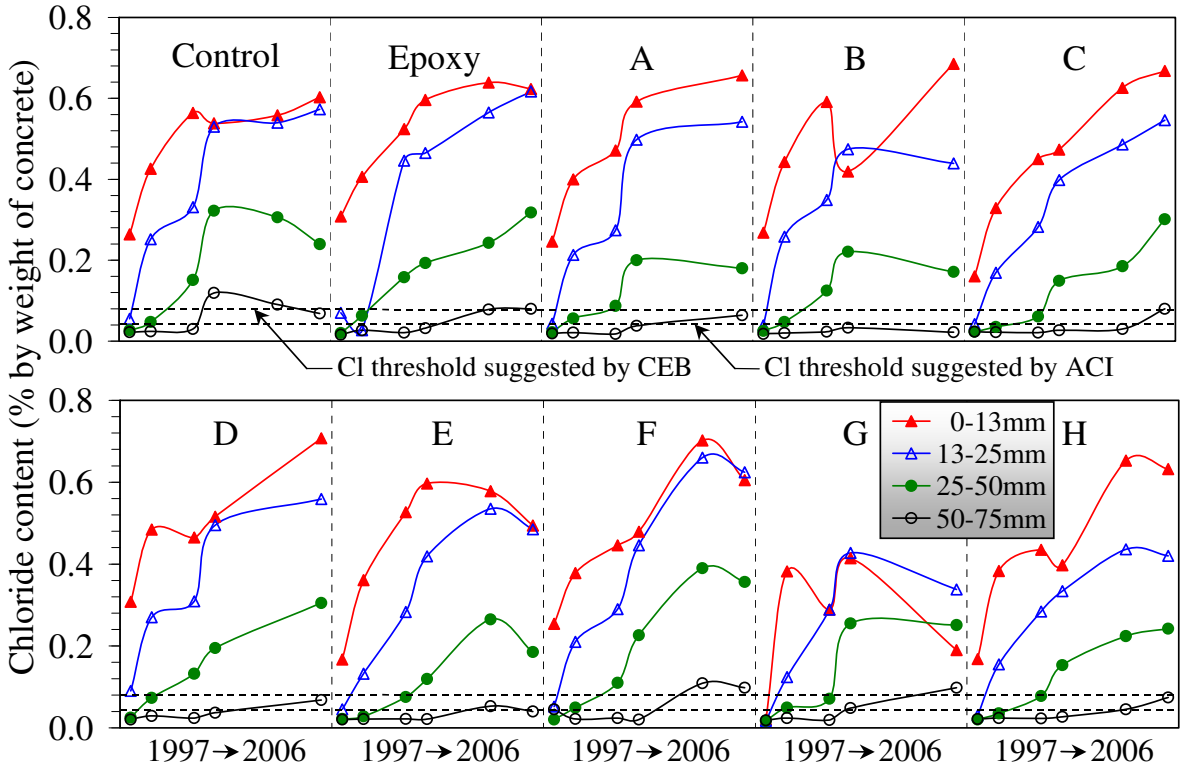

Fig. 4–Total chloride content measured in concrete cores from barrier walls (ASTM C114)

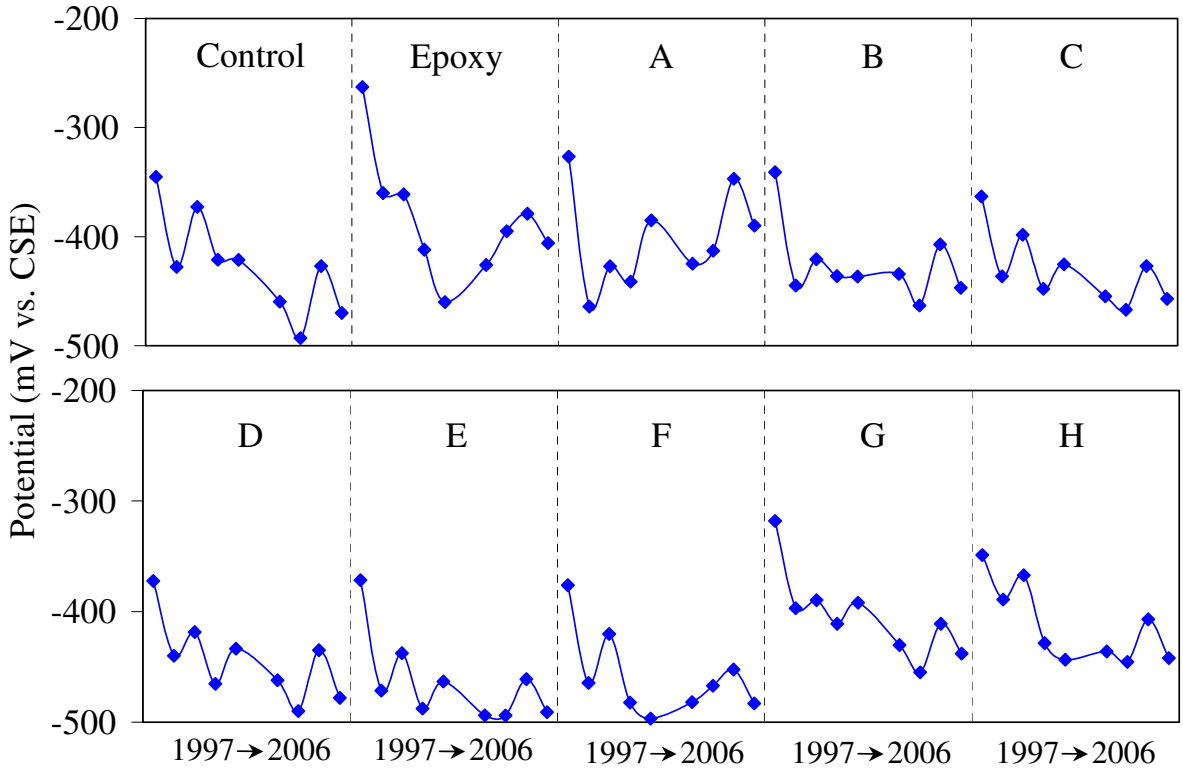

Fig. 5–Average half-cell potential measured over main reinforcement (ASTM C876)

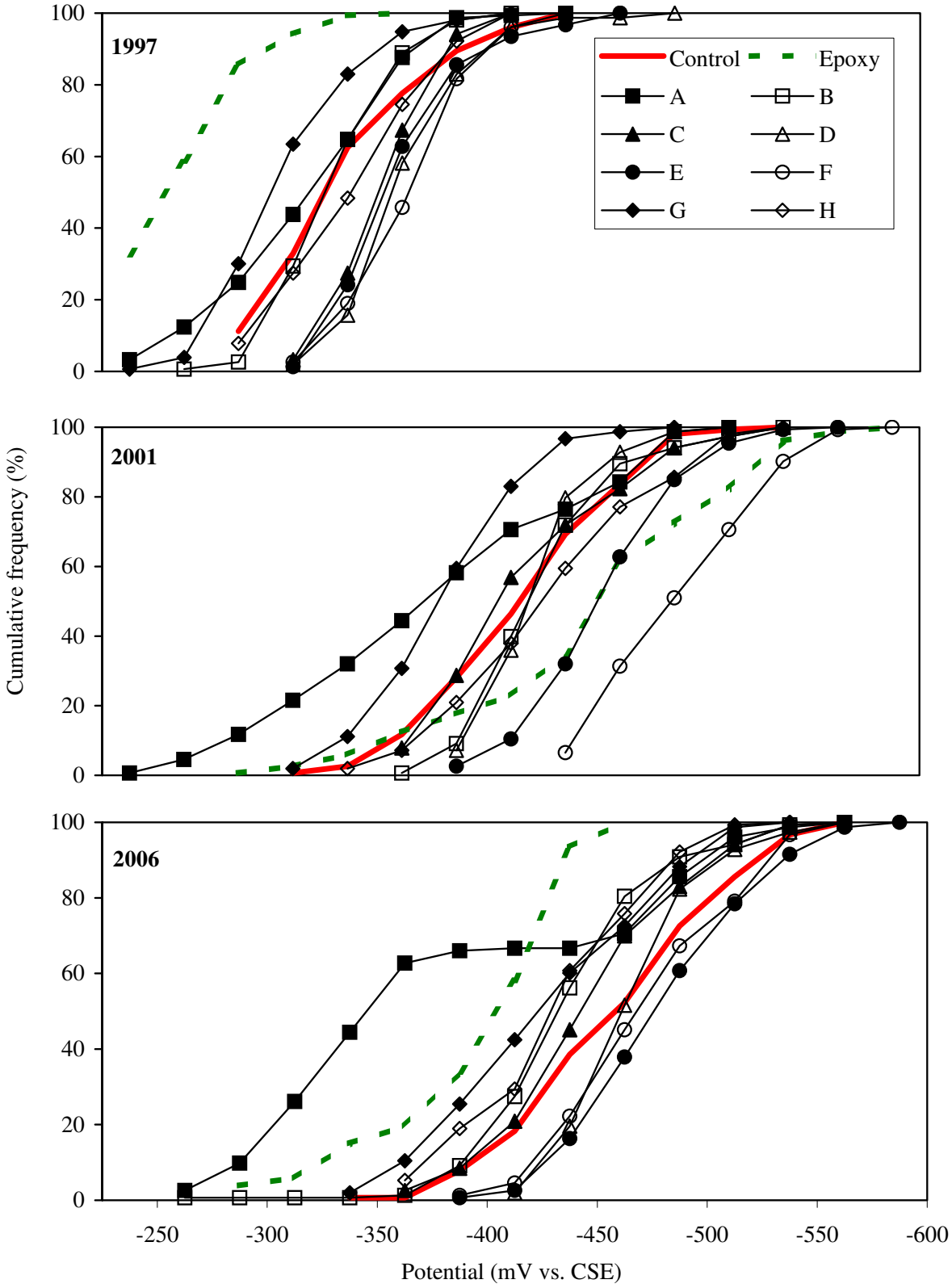

Fig. 6–Cumulative distributions of half-cell potential measured over main reinforcement

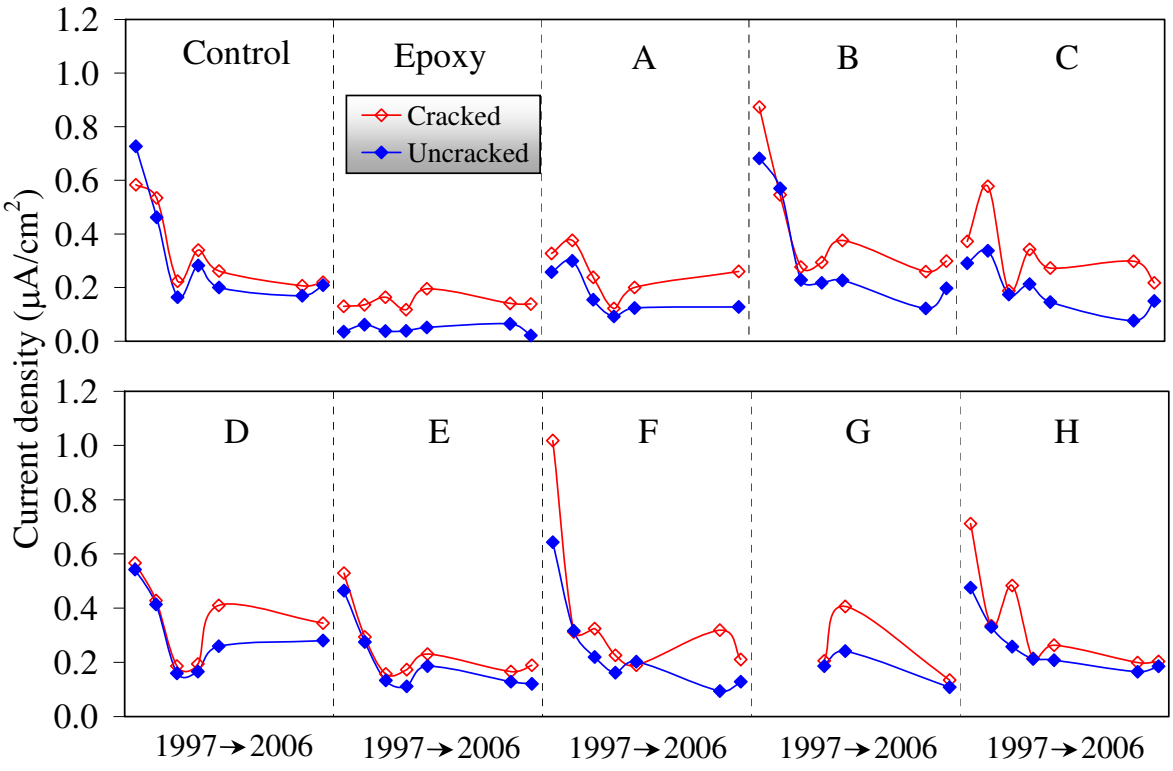

Fig. 7–Average corrosion rate measured over main reinforcement (1 μA/cm^2 = 6.45 μA/in.^{2})

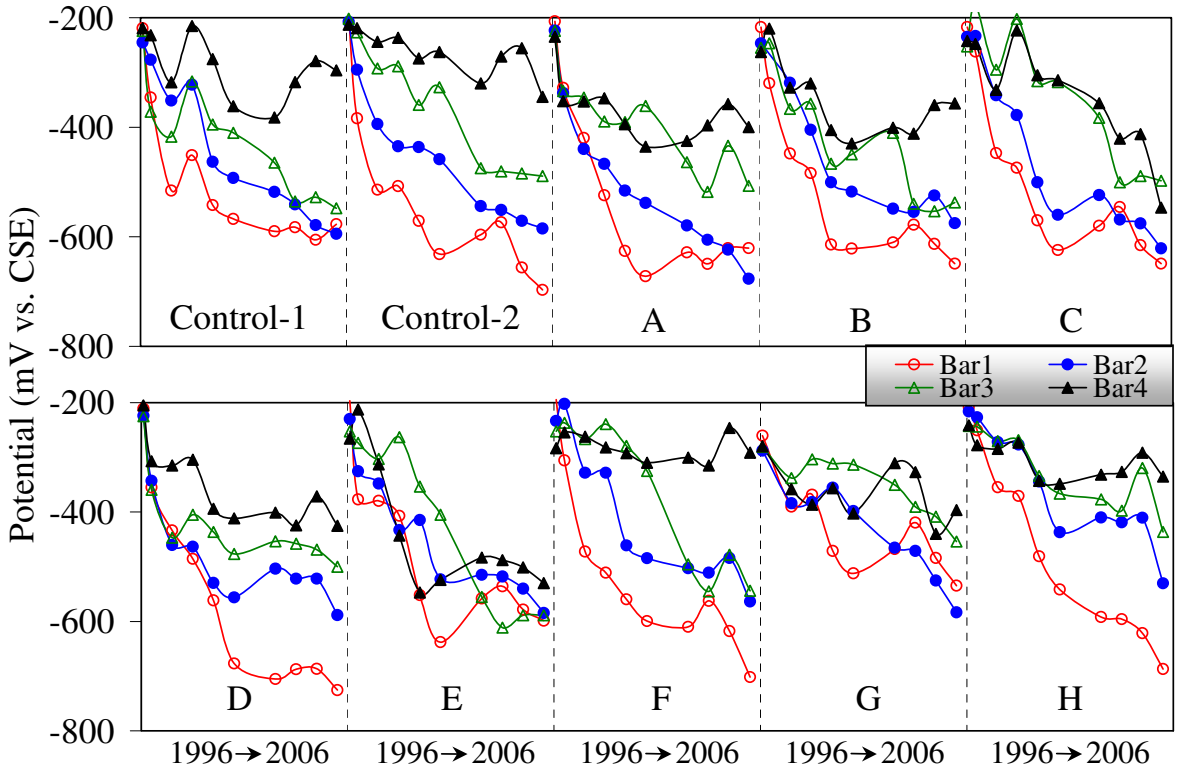

Fig. 8–Half-cell potential measured over embedded rebar ladders

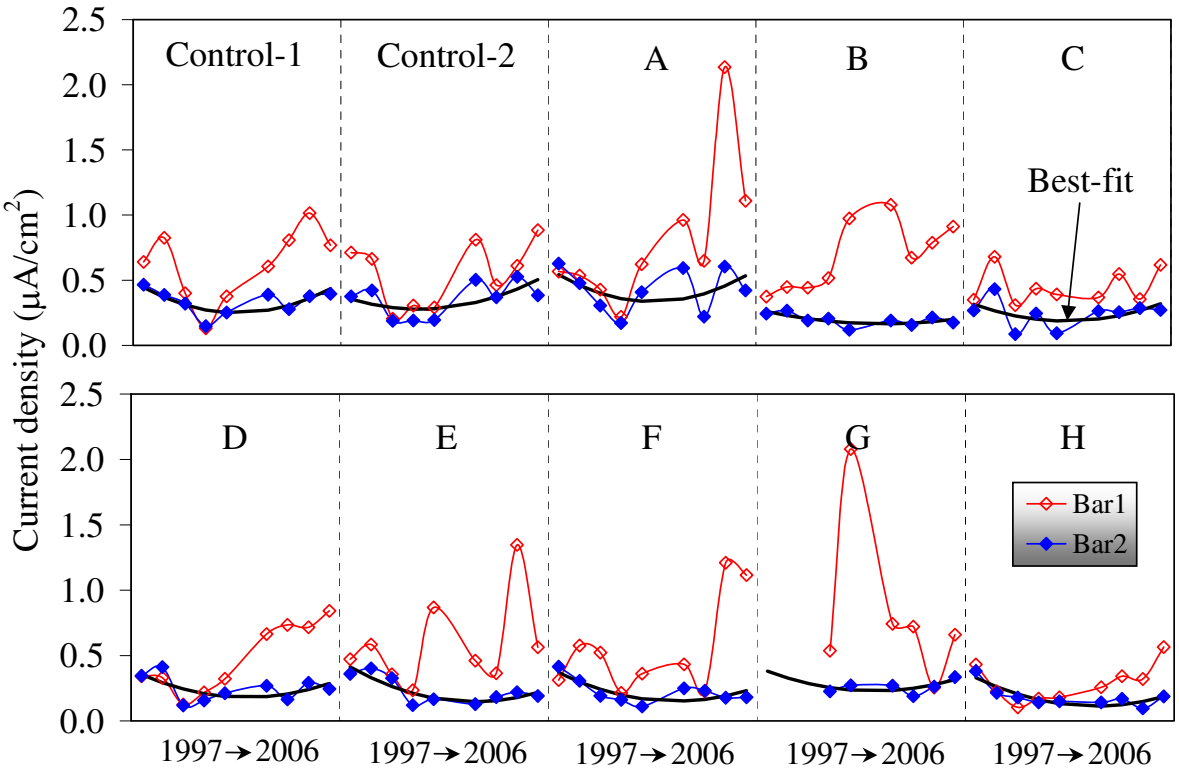

Fig. 9–Corrosion rate measured over embedded rebar ladders (1 μA/cm^2 = 6.45 μA/in.^{2})

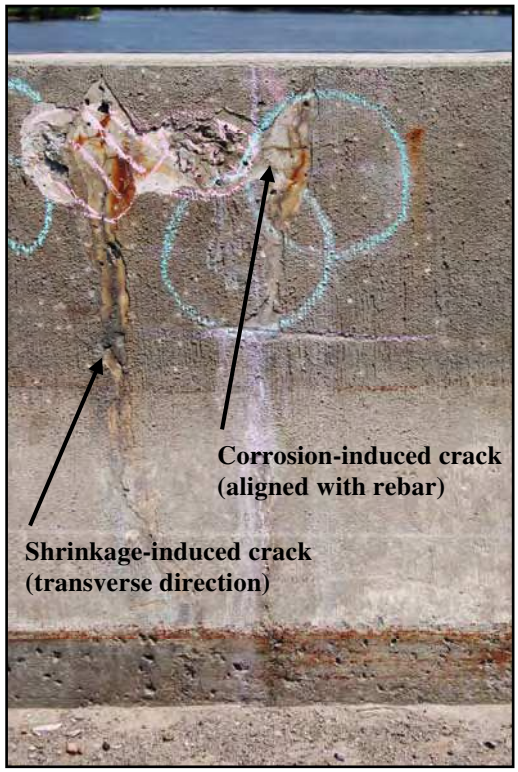

Fig. 10–View of barrier wall surface of control span in June 2006

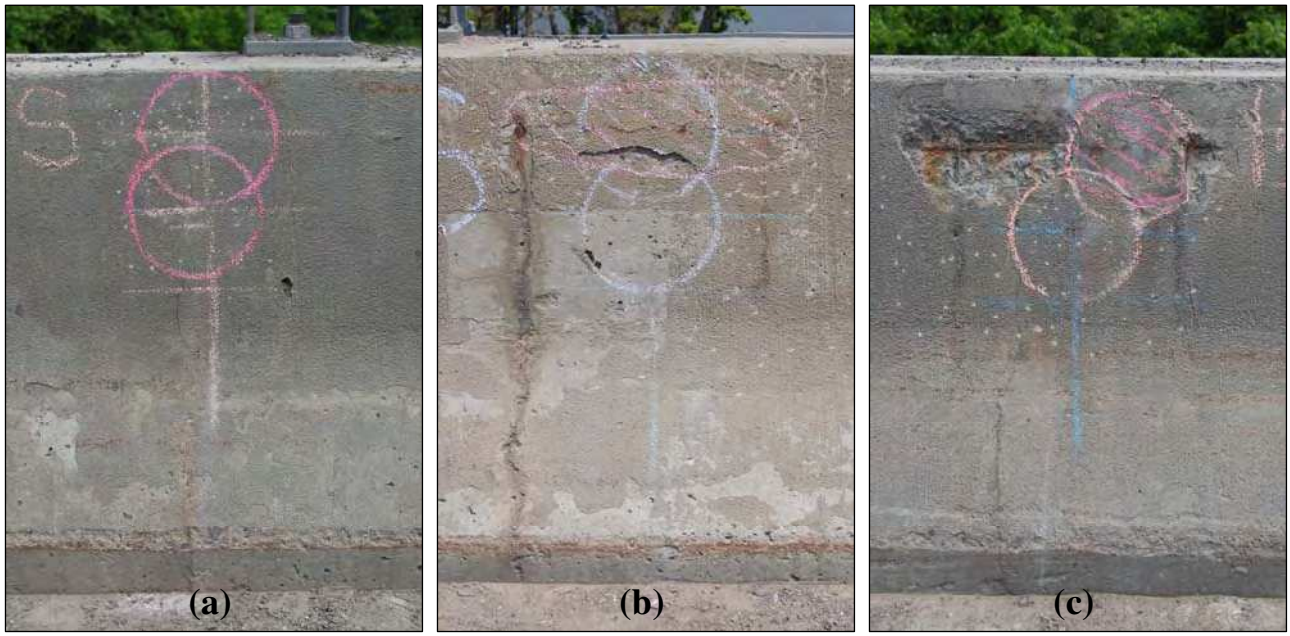

Fig. 11–View of barrier wall surface showing three typical levels of damage:
(a) cracking (span H), (b) cracking and delamination (span G), and (c) cracking, delam. and spalling (span C)